Modeling VLE and LLE of Deep Eutectic Solvents (DES) and Ionic Liquids (IL) Using PC-SAFT Equation of State. Part II

Ali Aminian*

ABSTRACT: This study aims to use Perturbed-Chain Statistical Associating Fluid Theory (PC-SAFT) to describe the phase behavior of systems containing DESs and ILs. The DESs are based on Tetrabutylammonium chloride ([N4444]Cl) and Tetrabutylammonium bromide (TBAB) as hydrogen bond acceptors, and levulinic acid (LevA) and Diethylene Glycol (DEG) as hydrogen bond donors in the mole ratio of 1:2 and 1:4, respectively. The predicted phase equilibrium data from PC-SAFT has been compared to those from COSMO-RS and NRTL predictions. ILs studied in this work are low viscosity ether-functionalized pyridinium-based ILs [E_nPy][NTf_2] and [C_mPy][NTf_2], while 1-(2-methoxyethyl)-1-methylpyrrolidiniumbis(trifluoromethylsulfonyl)-amide) ([COC_2mPYR][NTf_2]) and 1-propyl-3-methylimidazolium bis{trifluoromethylsulfonyl}imide ([Pmim][NTf_2]) were used for the study of the LLE systems with n-heptane + thiophene and n-hexane + ethylbenzene, respectively. In the last part, mixtures of linear alkanes and perfluoroalkanes have been studied to predict the phase behavior of perfluoroalkylalkanes with their linear alkane counterparts and comparisons have been made against SAFT-Mie pair potential.

Keywords: PC-SAFT; Deep Eutectic Solvents; Ionic Liquids; CO_2+CH_4 separation; VLE-LLE

1. Introduction

Separation of aromatic hydrocarbons from their mixtures with aliphatic hydrocarbons is an economical challenge, which chemical and petrochemical industries are facing and considering as a challenge. Since those mixtures form azeotropes, efficient separation and reuse of the solvent is not complete, therefore, researchers need green solvents with high selectivity toward one

component, which means it can be immiscible for other component [1]. On the other hand, extractive and azeotropic distillations still need huge amounts of energy to separate azeotrope-formed mixtures, which have disadvantages from the operation cost point of view. Thus, liquid-liquid extraction can be viewed as a viable alternative to other options with lower energy demand and smaller equipment size for separation, while it can utilize green solvents, which are not harmful to the environment because they are biodegradable [2]. The main advantage of using DESs and ILs in LLE processes is the fact that they can be recycled with minimum amount of energy consumption for recovery compared to other organic solvents. DESs and ILs possess negligible amount of vapor pressure and are stable over wide ranges of temperature, which means they can be easily separated from the extract phase and reused [3]. One of the most interesting properties of ILs and DESs is the tune-ability of their thermodynamic properties, like selective miscibility toward a substance; therefore, it has been estimated at least a billion such ILs or DESs. However, it is important to theoretically predict the phase behavior of mixtures containing DESs and ILs for design and optimization purposes, because experimentation over wide ranges of T and P is a crucial and expensive task.

Although amine absorption with chemical reaction is currently being used in several petrochemical industries to remove CO_2 from raw natural gas, however, loss of amine due to thermal or chemical degradation, equipment corrosion, and high energy demands during the regeneration have hindered the extensive use of amine absorption processes. A viable alternative for amine absorption would be the use of DESs or ILs, which are selective to absorb CO_2 over CH_4. For instance, N-methyl-2-hydroxyethylammonium propionate [m-2HEA][Pr], for pressures up to 200 bar, can be used for ideal CO_2/CH_4 selective separation in which low CH_4 solubility with negligible influence of temperature and high CO_2 solubility with high temperature influence can be observed [4]. Ramdin

et al. reported ideal CO_2/CH_4 selectivity for a number of ILs for pressures up to 14 MPa. They reported CH_4 solubility of 10-times lower than that of CO_2 at similar conditions [5]. Hojniak et al. [6] synthesized glycol functionalized ILs for membrane separations, which exhibited 2.3 times higher CO_2/N_2 and CO_2/CH_4 gas separation selectivities compared to analogous ILs. Zeng et al. [7] reported the selective separation of CO_2 from CH_4 by using ether-functionalized pyridinium-based ILs $[E_nPy][NTf_2]$ and compared the selectivities to those of non-functionalized analogues $[C_mPy][NTf_2]$, which showed highly selective separation of CO_2 from CH_4. Azole-based protic IL named as 1,5-diazabicyclo[4,3,0] non-5-ene 1,2,4-1H-imidazolide ([DBNH][1,-2,4-triaz]) has also been prepared by Zhang et al. to selectively separate H_2S and CO_2 from CH_4 [8].

On the other hand, it has been shown that fluorinated ILs are good candidate for CO_2 absorption, however, it would be a need for higher pressures for other formulations of ILs. For example, high pressure solubility of CO_2 in trihexyltetradecylphosphonium bromide [thtdp][Br], trihexyltetradecylphosphonium dicyanamide [thtdp][dca], and trihexyltetradecylphosphonium bis(2,4,4-trime-thylpentyl)phosphinate [thtdp][phos] have been reported for pressures up to 900 bar [9]. Therefore, in this work, tries have been made to model fluorinated ILs, which have high selectivity toward separation of CO_2 from CH_4 for pressures up to 30 bar.

Up to now, several thermodynamics models have been tested to capture the complex behavior of systems comprising associating molecules like DESs and ILs; among them NRTL, UNIQUAC, and UNIFAC are the most widely used models. In this context, PC-SAFT EoS is nearly young, and it is of interest to apply PC-SAFT formulation to newly developed systems composed of DESs and ILs. PC-SAFT model has been proved as a powerful thermodynamics model capable of accurate representation of binary and ternary mixtures composed of DESs and ILs [10]. For example, Al-fnaish and Lue [11] applied PC-SAFT modeling to methylimidazolium bis

(trifluoromethylsulfonyl) imide ionic liquids (ILs) ([$C_n$mim][NTf_2] where n=2, 4, 6, and 8)+CO_2 or H_2S over the temperature range of 290.95-414.92 K. Zubeir et al. [12] implemented PC-SAFT to model the vapor-liquid equilibria of binary system of lactic acid (LA)- tetramethylammonium chloride (TMA-Cl)/ tetraethylammonium chloride (TEA-Cl)/ tetrabutylammonium chloride (TBA-Cl) + carbon dioxide over the temperature range of 298.15-318.15 K. Also, solubility of carbon dioxide in toluene+ bis(trifluoromethylsulfonylimide) ([Tf_2N])-imidazolium/pyridinium/thiolanium/phosphonim as cations from 298.15 to 333.15 K modeled by Canales et al. [13]. Moreover, solubility of hydrocarbons, thiophene, or alcohols in 1-butyl-1-methylpyrrolidinium tetracyanoborate ([BMPYR][TCB]) has been considered [14].

Table 1 lists the experimental and modeling works with their respective ranges of temperature and pressure for different binary and ternary mixtures composed of DESs and ILs, namely, fluorinated and non-fluorinated ILs, and several types of DESs. As listed, it has been shown that both ILs and DESs are effective absorbents for CO_2 capture thanks to their molecular and ionic constitutions, which might be regulated to have high affinity and selectivity toward CO_2 in a mixture of CO_2+CH_4. Therefore, CO_2 solubility data and accurate modeling approaches are required for design and optimization purposes. To design a perfect mixture of neat constituent components for ILs or DESs, COSMO formulation can be used to have a proper match between interacting surfaces of CO_2 molecules and absorbent molecules independent of experimental data, but the sigma-profile of several ILs and DESs are not as yet reported in the literature. On the other hand, molecular-based thermodynamics models like SAFT-family equations can capture the complex interaction of ionic interactions in a solution. The main advantage of the PC-SAFT EoS compared to local composition activity coefficient models may be due to the fact that the latter models need extensive experimental data to correlate the large numbers of binary interaction parameters of those models;

but in case of ILs and DESs, the only required experimental data for regression would be the liquid phase density of the pure components, which is useful for high pressure phase equilibria calculations.

Table 1. Summaries of experimental and modeling studies for different binary and ternary mixtures composed of DESs and ILs

System	DES or IL	Molar ratio	Temperature range, K	Methodology	Ref.
n-heptane + toluene	Tetrabutylammonium chloride ([N4444]Cl)-levulinic acid (LevA) Choline Chloride ([Ch]Cl)-LevA BenzylCholine Chloride ([BzCh]Cl)-LevA	1:2	298.15-353.15	Experimental /COSMO-RS regression	[15]
n-hexane + thiophene n-octane + thiophene	tetrahexylammonium bromide-ethylene glycol tetrahexylammonium bromide-glycerol	1:2	298.15	Experimental /NRTL regression	[16]
n-heptane + toluene	Ethyltriphenylphosphonium iodide-Ethylene glycol (EG) Ethyltriphenylphosphonium iodide-Sulfolane	1:6	333.15	Experimental /NRTL regression	[17]
Ethylbenzene+styrene	tetrabutyl ammonium bromide (TBAB)-EG TBAB-Diethylene glycol (DEG) TBAB-Triethylene glycol (TEG)	1:4	298.15	Experimental /NRTL and COSMO-RS regressions	[18]
n-heptane + toluene cyclohexane + toluene n-hexane + toluene	[EMim][NTf_2] and [EMpy][NTf_2]	-	298.15	Experimental /NRTL regression	[19]
n-hexane + ethylbenzene cyclohexane + ethylbenzene	$BMimMSO_4$ $BMimNTf_2$ $PMimNTf_2$	-	298.15	Experimental / COSMO-RS regression	[20]
n-octane + benzene cyclooctane + benzene n-nonane + benzene n-nonane + Toluene	$BMimMSO_4$ $BMimNTf_2$	-	298.15	Experimental / COSMO-RS regression	[21]
thiophene+hexadecane thiophene+n-octane	1,3-Dihydroxyimidazolium bis{(trifluoromethyl) sulfonyl}imide, [OHOHIM][NTf_2], 1-Butyl-3-methylimidazolium trifluoromethanesulfonate, [BMIM][OTf]	-	308.15	Experimental /NRTL regression	[22]
Thiophene+n-hexane	methyltriphenylphosphonium bromide (MTPPBr)/ glycerol/ ethylene glycol tetraethylammonium chloride (TEACl)/ glycerol/ ethylene glycol	1:3 1:2	298.2	Experimental / COSMO-RS regression	[23]
n-Hexane + ethanol n-heptane + 1-butanol n-heptane + 2-butanol	[Ch]Cl-LevA [Ch]Cl-EG [Ch]Cl-phenol	1:2	298.15	Experimental / PC-SAFT binodal curve regression	[24]
Thiophene+octane	TEACl-EG TEACl-Glycerol MTPPBr-EG MTPPBr- Glycerol	1:2 1:3	298.15	Experimental / PC-SAFT regression	[25]

SAFT-family modeling have also been used to model the phase equilibria of binary mixtures of perfluoroalkanes and alkanes. Mccabe et al. [26] used SAFT-VR to predict the high-pressure phase

equilibria of binary mixtures of perfluoromethane + (n)-alkanes from methane to heptane. Morgado et al. [27] employed SAFT-γ Mie group-contribution approach for modeling the fluid-phase equilibria of mixtures of n-alkanes + n-perfluoroalkanes, namely, n-hexane + n-perfluorohexane and n-butane + n-perfluorobutane systems at different temperatures. Aparicio [28] calculated Phase equilibria of perfluoroalkane + alkane binary systems comprising perfluoromethane + methane or ethane, perfluoropropane + propane, and perfluorobutane + butane, but they can not be sued for accurate prediction of the phase equilibria, as they accompanied with significant deviations from experimental data for the whole temperature ranges. Binary mixtures of alkanes and perfluoroalkanes exhibit large positive deviations from Raoult's law and large positive excess volume and enthalpy owing to the uncommon weak hydrophobic attractive interactions between hydrocarbon (HC) and fluorocarbon (PFC). Therefore, the anomalous phase behavior of PFC+HC binary mixtures near ambient conditions is hard to model, and predicting the liquid-liquid immiscibility regions of these components is a crucial task. Although, application of SAFT formulation for modeling VLE of perfluoroalkanes and alkanes systems thus far have been reported [26-28], but there is still room for further research to use PC-SAFT formulation for these systems to increase the modeling accuracy.

In this work, we are trying to evaluate the capability of the PC-SAFT to predict the phase equilibrium of ternary mixture containing DES and ILs. Furthermore, the formulation was extended to the binary mixtures containing ILs and the mixtures of normal alkanes with perfluoro-n-alkanes. The comparison was made against NRTL, COSMO-RS, SAFT-VR, and SAFT-γ Mie models in order to examine the accuracy and applicability of the proposed PC-SAFT model for the systems considered in this study.

2. PC-SAFT modeling for VLE and LLE calculations

SAFT-family equations are developed based on the molar Helmholtz free energy, which is defined as the summation of the residual molar Helmholtz free energy and the ideal gas molar Helmholtz free energy at constant temperature and molar density [29],

$$A|_{T,\rho} = A^{res}|_{T,\rho} + A^{ig}\big|_{T,\rho} \tag{1}$$

where A is the molar Helmholtz energy, T is the absolute temperature, and ρ is the total molar density. The residual and the ideal gas molar Helmholtz free energies can be individually defied as follow,

$$A^{res} = A^{hc} + A^{disp} + A^{Assoc} + A^{polat} \tag{2}$$

$$A^{ideal} = \sum x_i \, ln \, \rho_i \Lambda_i^3 - 1 \tag{3}$$

Reader can refer to the references further details on the derivation of the equations of PC-SAFT [29]. The PC-SAFT pure-component parameters for non-associating and associating compounds were obtained by minimizing the differences between the experimental and calculated values of the liquid density (ρ) and the vapor pressure (p^{sat}) data,

$$OF = min \sum_i^N \left(\left| \frac{\rho_i^{exp} - \rho_i^{calc}}{\rho_i^{exp}} \right| \right) + \sum_i^N \left(\left| \frac{p_i^{sat^{exp}} - p_i^{sat^{calc}}}{p_i^{sat^{exp}}} \right| \right) \tag{4}$$

where N denotes the number of the experiment data.

The pure-component parameters of the DESs and ILs were determined by minimizing the following objective function, as both DESs and ILs possess negligible amounts of vapor pressure,

$$OF = min \sum_i^N \left(\left| \frac{\rho_i^{exp} - \rho_i^{calc}}{\rho_i^{exp}} \right| \right) \tag{5}$$

In the next section, the molecular modeling methodology, pure-component parameters of the PC-SAFT model, and the percentage errors of the fitting algorithm have been reported.

3. Molecular model of the compounds

The DESs and ILs were considered as compounds composed of two ionic species, by which neutral ionic pairs formed. Cations and anions of the DESs and ILs are associated together, while $A_1 \ldots B_1$ association interactions between anion and cation parts were merely allowed. The strength of association $A_1 \ldots B_1$ is characterized by the PC-SAFT association parameters ($\varepsilon_{A,B}$ and $K_{A,B}$) and the number of associating sites per molecule. It seems two association sites (2B scheme), which were applied to the DESs and ILs, can reasonably predicts DES and IL densities at different pressures and temperatures, as reported by other researchers [10, 32].

Non-associating compounds without dipolar interactions require only three pure-component parameters, namely, the segment number of molecule *i* (m_i), the temperature-independent segment diameter of molecule *i* (σ_i), and the dispersion-energy parameter of molecule *i* (u_i/k). Associating compounds need two additional parameters of the association contributions: 1- the effective volume of association ($K_{A,B}$), and 2- the association energy parameter ($\varepsilon_{A,B}$). In case of DESs, the ratio specific individual constituent approach was taken into account, because molar ratios of hydrogen bonding donor and hydrogen bonding acceptor parts are different from each other. In a mixture of two associating compounds, the cross-associating interactions were obtained according to the Wolbach and Sandler equations. In this work, no induced association were considered between a self-associating component and a non self-association component.

Furthermore, CO_2, thiophene, n-alkanes, and perfluoro-n-alkanes molecules were modeled as non-associating fluids, as they do not show self- and/or cross association interactions. Thus, they require three pure-component parameters *m,* σ, and *u/k*, which were taken from Gross and Sadowski [29, 30]. Dipolar interactions were considered for perfluoroalkanes due to their values of dipole moment (~3D).

Also, binary interaction parameter k_{ij} is an adjustable parameter that can be used to increase the correlation between predicted and actual values by fitting to experimental VLE or LLE data. Therefore, we have used regressed-k_{ij} values for each pair of fluids. The k_{ij} values were found based on the nonlinear least squares method by using Levenberg Marquardt algorithm with the initial values of $k_{ij} = 0$. Percentage average absolute relative deviation (ARD%) was used to monitor the performance of the PC-SAFT model versus real data,

$$ARD = \frac{100}{N}\sum_{i}^{N}\frac{\left|X_i^{exp} - X_i^{calc}\right|}{X_i^{exp}} \tag{6}$$

where X is vapor mole fraction, total pressure, liquid density (ρ), or vapor pressure (p^{sat}) and N denotes total number of experimental data.

Tables 2 and 3 show the PC-SAFT pure-component and the temperature-dependent or independent binary interaction parameters for all substances presented in this study, respectively. As shown, the references of the experimental data were provided for the VLE, LLE, pure density, or pure vapor pressure data. Supplementary Material associated with this research article shows the prediction performance of the proposed PC-SAFT model for the density-pressure, density-temperature, and vapor pressure curves in comparison to the available experimental data for the whole pure components under consideration.

Table 2. PC-SAFT pure-component parameters- $ARD\rho\%$ and $ARDp^{sat}$ are percentage average absolute deviation for predicting the liquid density and vapor pressure of the pure components.

Component	M(-)	σ(Å)	ε/k_B (K)	K^{AB}	ε^{AB}/k	μ(D)	x_p	$ARD\rho(\%)$	$ARDp^{sat}$ (%)	Ref
TBAB/DEG (1:4)	2.131	4.772	961.8	1×10^{-6}	5000			0.0449		this study
[N4444]Cl/LevA	2.842	4.672	865.10	1×10^{-6}	5000			0.207		
[Pmim][NTf_2]	8.85	3.623	336.50	0.01	5000			0.134		
[COC_2mPYR][NTf_2]	8.049	3.808	327.66	0.01	4000			2.097		
[E_1Py][NTf_2]	2.937	5.440	767.07	1×10^{-6}	5000			0.0041		
[E_2Py][NTf_2]	2.950	5.685	793.45	1×10^{-6}	5000			0.0024		
[E_3Py][NTf_2]	2.953	5.903	790.39	1×10^{-6}	5000			0.0016		

$[C_4Py][NTf_2]$	7.824	3.763	254.08	0.01	5000			1.221		
$[C_7Py][NTf_2]$	2.900	5.854	803.36	1×10^{-6}	5000			0.003		
$[C_{10}Py][NTf_2]$	2.921	6.115	790.49	1×10^{-6}	5000			0.002		
Styrene	3.122	3.694	294.05					0.613	1.748	
C_4F_{10}	3.701	3.554	165.53			2.45	-	1.956	0.613	
Thiophene	2.348	3.562	303.01					0.086	0.565	32
C_6F_{14}	4.554	3.757	177.43			2.94	0.05	0.797	4.908	32
C_4H_{10}	2.331	3.708	222.88							29
C_6H_{14}	3.057	3.798	236.77							29
C_7H_{16}	3.347	3.851	243.67							29
CO_2	2.072	2.785	169.21							29
CH_4	1.000	3.704	150.03							29
Toluene	2.756	3.734	289.52							29
Ethylbenzene	3.079	3.797	287.35							29

Table 3. Binary interaction parameters regressed to the experimental LLE or VLE data.

System	k_{ij}	Ref. for Exp. LLE/VLE data	Ref. for Exp. pure density data (1)	Ref. for Exp. pure vapor pressure data (1)
TBAB/DEG (1:4)+Styrene	0.015105	[18]		
TBAB/DEG (1:4)+Ethylbenzene	0.002922			
Styrene (1)+Ethylbenzene(2)	-0.008862		[33-35]	[34,36]
[N4444]Cl/LevA (1:2) (1)+Toluene (2)	-0.023627	[15]	[15]	
[N4444]Cl/LevA (1:2)+n-Heptane	-0.038571			
Toluene + n-Heptane	0.011027			
$[Pmim][NTf_2]$ (1)+n-Hexane (2)	0.00780	[20]	[37]	
$[Pmim][NTf_2]$+Ethylbenzene	-0.00522			
Ethylbenzene+n-Hexane	0.01319			
$[COC_2mPYR][NTf_2]$ (1)+Thiophene (2)	0.014923	[38]	[39]	
$[COC_2mPYR][NTf_2]$+n-Heptane	0.04743			
Thiophene+n-Heptane	0.041873			
$[E_1Py][NTf_2]$ (1)+CO_2 (2)	0.179	[7]	[7]	
$[E_2Py][NTf_2]$ (1)+CO_2 (2)	0.209			
$[E_3Py][NTf_2]$ (1)+CO_2 (2)	0.220			
$[E_1Py][NTf_2]$ (1)+CH_4 (2)	0.730-0.7750×T			
$[E_2Py][NTf_2]$ (1)+CH_4 (2)	0.890-0.925×T			
$[E_3Py][NTf_2]$ (1)+CH_4 (2)	0.9960-0.9990×T			
$[C_4Py][NTf_2]$ (1)+CO_2 (2)	0.0570	[7]	[7]	
$[C_7Py][NTf_2]$ (1)+CO_2 (2)	0.2260			
$[C_{10}Py][NTf_2]$ (1)+CO_2 (2)	0.2480			
$[C_4Py][NTf_2]$ (1)+CH_4 (2)	0.9850-0.9120×T			
$[C_7Py][NTf_2]$ (1)+CH_4 (2)	0.660-0.70×T			
$[C_{10}Py][NTf_2]$ (1)+CH_4 (2)	0.9450-0.960×T			
C_6F_{14} (1)+C_6H_{14}(2)	0.12808-0.05087×T			
C_4F_{10} (1)+C_4H_{10} (2)	0.08807-0.00414×T	[40]	[41,42]	[41,42]

4. Results and discussion

Experimental LLE and VLE data were taken from different references [7,15,18,20,38,40]. Tables 2 and 3 show the pure-component parameters of the PC-SAFT model and temperature-dependent or independent binary interaction parameters (k_{ij}) of the systems, respectively.

4.1. Modeling LLE of the ternary system of ethylbenzene + styrene + TBAB/DEG (1:4).

Separation of styrene from its mixture with unreacted ethylbenzene is found to be effective by using TBAB/DEG since it can be reused without appreciate lost, while it is selective toward styrene and is environmentally friendly. Due to low conversion efficiency of the reaction, mole fraction of liquid styrene ranges between 0.0 to 0.5 and conventional distillation separation can not play much role, as the mixture is composed of close boiling components. Therefore, LLE modeling of ethylbenzene + styrene with TBAB/DEG (1:4) is of great importance [18].

Experimental LLE data of this system were collected from [18], and the system triangular phase diagram is shown in Figure 1. PC-SAFT pure-component parameters for ethylbenzene is reported by Gross and Sadowski [29], while styrene and TBAB/DEG (1:4) PC-SAFT pure-component parameters were developed in this work by fitting to the experimental vapor pressure and liquid density data. Table 2 shows the PC-SAFT pure-component parameters and the percentage absolute relative deviations related to the vapor pressure and liquid density data correlations, according to E. (36).

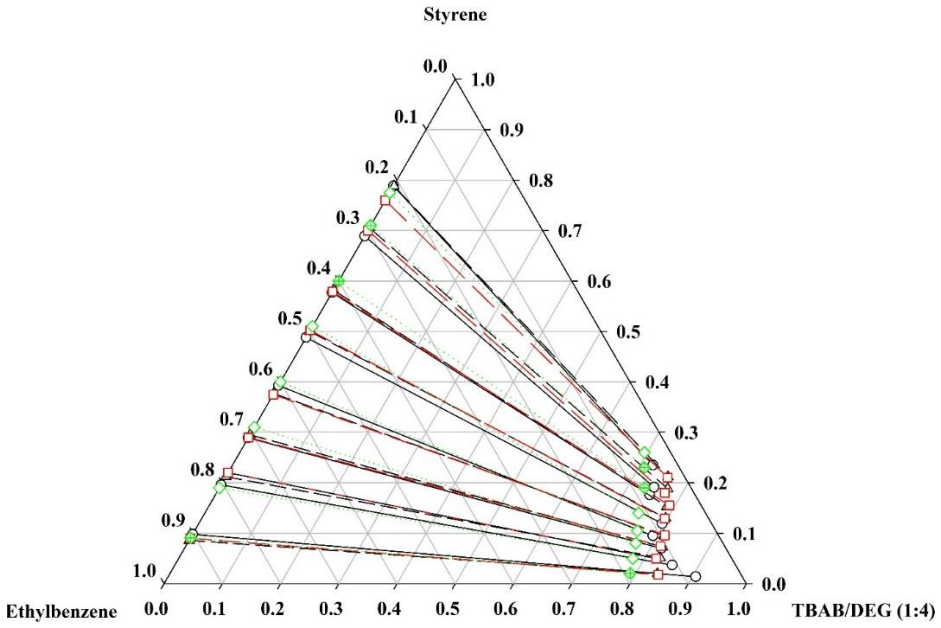

Figure 1. LLE data for the system of ethylbenzene + styrene with TBAB/DEG (1:4).

Comparison between the experimental [18] (solid black lines with open circles) and calculated

compositions by PC-SAFT (dashed black lines open triangles), NRTL [18] (dashed red lines with open squares), and COSMO-RS [18] (dotted green lines with open diamonds) at T=298.15 K and P=101.3 kPa.

In case of TBAB/DEG, Rackett formulation [43] was used for predicting the liquid density data, and then PC-SAFT pure component parameters were found by fitting to the predicted liquid density data. Supplementary Material contains the comparisons between actual and predicted values of the vapor pressure and liquid density data (Figures S1-3).

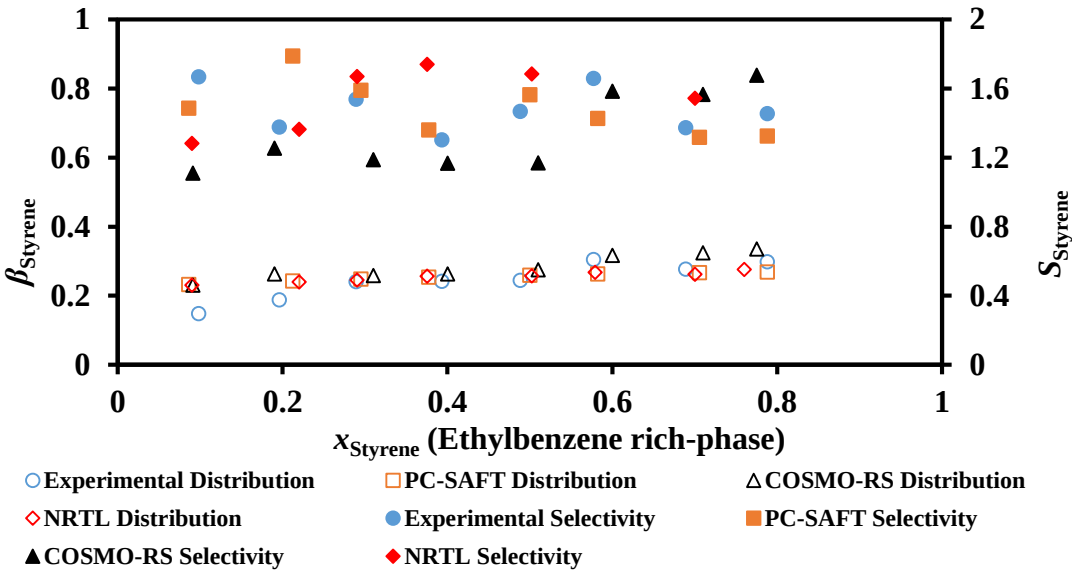

Figure 2. Comparison between the experimental [18] and calculated distribution coefficient and selectivity by PC-SAFT, NRTL, and COSMO-RS models as a function of styrene mole fraction in ethylbenzene rich-phase (T=298.15 K, P=101.3 kPa).

2B association scheme, by which only A…B association is allowed, was considered for the DES molecules. Furthermore, binary interaction parameters k_{ij} were obtained by correlating to the experimental ternary LLE data of the system [18]. Because the tie lines slope downward from the ethylbenzene side toward the TBAB/DEG side, thus styrene has higher concentration in ethylbenzene, as indicated by the small negative value of the k_{ij} between ethylbenzene and styrene.

Therefore, at equilibrium, accumulation of considerable amount of ethylbenzene in the extract layer is probable. As revealed in Figure 2, for the distribution coefficients (β) and selectivities (S) associated with the DES (Eqs. 7 & 8), TBAB/DEG gives low distribution coefficients (maximum of 0.305), as there might be a need for a large amount of solvent, while β values are almost constant over the entire ranges of styrene mole fraction in the ethylbenzene-rich phase, however, S values higher than unity, maximum of 1.667, proves the appropriateness of the solvent to remove styrene from ethylbenzene. Compared to ethylbenzene + styrene + [BzMIM][DCA] system [44], which has higher β and S values (up to 0.68 and 2.81, respectively), economic analysis should be performed in terms of capital and operational costs to make a selection between IL or DES, as extracting agent.

As shown in Figures 1 and 2, comparisons have also been made against NRTL and COSMO-RS models for modeling the LLE of ethylbenzene + styrene + TBAB/DEG (1:4) [18]. Root Mean Square Deviation (RMSD) of the PC-SAFT, NRTL, and COSMO-RS models are 1.878%, 1.9%, and 3.9%, respectively (Eq. 9). Moreover, ARD for the β and S values are 15.886%/10.267%, 15.093%/12.132%, and 19.663%/16.219% for PC-SAFT, NRTL, and COSMO-RS models, respectively. The main disadvantage of NRTL model is that it needs three adjustable parameters for every binary system, while the third parameter is arbitrary chosen and has not physical meaning. Similarly, although COSMO-RS model is independent of experimental data, it suffers from the computational cost, as the basis set might have great influence on the accuracy of the generated sigma-profile; while the more complex basis set increases the demand for more time of computation. On the other hand, PC-SAFT model needs only five pure-component parameters, which can be obtained by fitting to the vapor pressure and/or liquid density data. Although it is based on the molecular interaction and fluid association theory, but accuracy of the experimental

data, binary interaction parameters, and selection of the association scheme might influence the accuracy of the PC-SAFT. From the error analysis, it seems both PC-SAFT and NRTL gave similar results, while COSMO-RS has less accuracy compared to other two models.

4.2. Modeling LLE of the ternary system of heptane + toluene + [N4444]Cl/LevA

Experimental LLE data for the ternary system of heptane + toluene + Tetrabutylammonium chloride/levulinic acid ([N4444]Cl/LevA) were gathered from Gouveia et al. [15]. Experimental density data of ([N4444]Cl/LevA in the range of 293.15 K to 353.15 K [15] was used to regress the PC-SAFT pure-component parameters of the DES. The $ARD\rho$ of 0.2075% shows the accuracy of the PC-SAFT to model the LLE of the system. The values of 1×10^{-6} and 5000 (K) for association volume ($K_{A,B}$) and energy ($\varepsilon_{A,B}$) interaction parameters similar to ILs were used in this study [45]. Predicted liquid density data of DES versus temperature can be seen in the Supplementary Material (Figure S4). PC-SAFT pure-component parameters of n-heptane and toluene were taken from [29]. Distribution coefficient (β) and selectivity (S) of the DES, to extract toluene from n-heptane, were used to make appropriate comparisons with COSMO-RS model against experimental data,

$$\beta_{toluene} = \frac{x_{toluene}^{DES\ rich-phase}}{x_{toluene}^{heptane\ rich-phase}} \tag{7}$$

$$S = \left(\frac{x_{toluene}^{DES\ rich-phase}}{x_{toluene}^{heptane\ rich-phase}}\right)\left(\frac{x_{heptane}^{heptane\ rich-phase}}{x_{heptane}^{DES\ rich-phase}}\right) \tag{8}$$

where $x_{toluene}^{DES\ rich-phase}$, $x_{toluene}^{heptane\ rich-phase}$, $x_{heptane}^{DES\ rich-phase}$, and $x_{heptane}^{heptane\ rich-phase}$ are toluene and n-heptane mole fractions in DES and heptane rich-phase, respectively. The higher β and S values means the ability of solvent to preferentially extract toluene from n-heptane, which is important from operation cost point of view. Figure 3 shows β and S values of experimental data [15], PC-SAFT, and COSMO-RS at 298.15 K and 101.3 kPa. As can be seen, PC-SAFT model represents experimental distribution coefficient and selectivity of the DES to extract toluene from

n-heptane better than COSMO-RS model. ARD of the β and S values of PC-SAFT and COSMO-RS models are 19.419%/21.272% and 30.619%/121.207%, respectively.

Modeling of the LLE data at 298.15 K and 101.3 kPa were performed using PC-SAFT model and comparisons have been made against COSMO-RS, as shown in Figure 4. RMSD was implemented to compare the performance of the PC-SAFT and COSMO-RS models, which is as follows,

$$RMSD = 100\sqrt{\sum_i \sum_n \left(x_{i,n}^{exp,I} - x_{i,n}^{calc,I}\right)^2 + \left(x_{i,n}^{exp,II} - x_{i,n}^{calc,II}\right)^2 / N} \quad (9)$$

where x is the mole fraction of the i-th component (i=1,2,and3) and summation is over the whole tie-lines (total of n) connecting mole fraction of phases I and II. Superscripts *exp*. and *calc*. represent experimental and calculated mole fractions, respectively, and N denotes total number of experimental data. Although COSMO-RS provided qualitative prediction of the experimental LLE data, but it has RMSD of 3.918%, while it is a predictive approach that uses just the sigma-profile of the pure components to calculate the activity coefficients, which is quite useful from LLE modeling view point. RMSD of 3.457% was obtained by the PC-SAFT model. As can be seen from Figure 3, the DES can be used as extracting agent for the separation of an aromatic compound from an aliphatic compound (selectivity higher than unity).

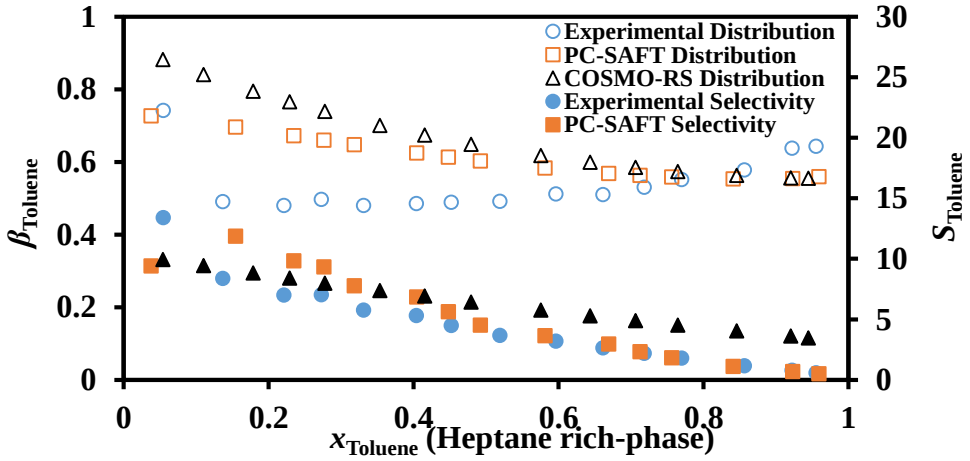

Figure 3. Comparison between the experimental [15] and calculated distribution coefficient and selectivity by PC-SAFT and COSMO-RS [15] models as a function of toluene mole fraction in n-heptane rich-phase (T=298.15 K, P=101.3 kPa).

Distribution coefficients far from unity means huge requirements for solvent, however, DES can be recycled and reused for multiple times. Increasing toluene concentration in the n-heptane rich-phase will decrease the selectivity, which translates into the decline in the efficiency of the DES to extract toluene from n-heptane, but DES is useful for the whole ranges of feed composition. Toluene is an aromatic that can act as an electron donor in dispersion interactions with DES. In this study, temperature-independent binary interaction parameters were implemented for the ternary system of n-heptane + toluene + [N4444]Cl/LevA, as shown in Table 3. As can be seen, toluene has higher interaction with DES in the PC-SAFT formulation framework (lower negative binary interaction parameter). In case of n-heptane + toluene due to unlike interactions, a positive binary interaction parameters was used.

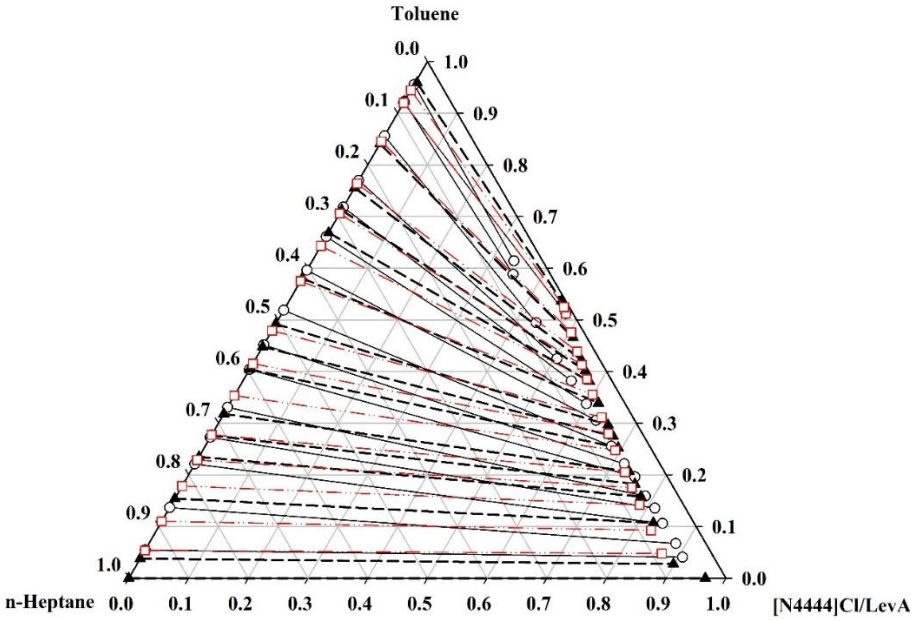

Figure 4. LLE data for the system of n-heptane + toluene + [N4444]Cl/LevA. Comparison between the experimental [15] (solid black lines) and calculated compositions by PC-SAFT

(dashed black lines) and COSMO-RS [15] models (dashed red lines) at T=298.15 K and P=101.3 kPa.

4.3. Modeling LLE of the ternary system of hexane + ethylbenzene + [Pmim][NTf_2]

LLE experimental data for the ternary systems hexane + ethylbenzene + 1-propyl-3-methylimidazolium bis{trifluoromethylsulfonyl}imide, [Pmim][NTf_2], at T=298.15 K and P=101.3 kPa were taken from Ref. [20]. Ethylbenzene distribution ratio (β) and selectivity parameter (S) obtained by PC-SAFT and COSMO-RS models were compared with experimental ones in Figure 5. ARD of 4.044% and 8.207% were obtained for β and S by using PC-SAFT approach, respectively, while error values of COSMO-RS model are 52.110% and 13.312%, respectively. Low β-values of the distribution coefficient of the system can not impose serious problem, as solvent can be recovered and reused multiple times, while selectivity values address the goodness of [Pmim][NTf_2] to selectively separate ethylbenzene from its mixture with n-hexane. Both β and S values decrease as a function of ethylbenzene in the n-hexane rich-phase, which indicates a decline in the mass transfer coefficient. Comparisons between PC-SAFT and COSMO-RS models to predict the LLE of this system is shown in Figure 6. As can be seen, PC-SAFT model has higher accuracy compared to the latter case with the RMSD value of 1.039%, while COSMO-RS model gives RMSD of 6.945%. Although COSMO-RS does not rely on the experimental LLE data, however, it needs sigma-profile of the components, which is a computationally expensive task. On the other hand, PC-SAFT model is based on the statistical thermodynamics theory that can capture the molecular interactions in the system, while it might need binary interaction parameters to enhance the accuracy of the modeling. From binary interaction coefficients in Table 3, one can see the strong interactions between ethylbenzene and

IL as a result of the electron donating characteristics of the ethyl functional group on the ethylbenzene.

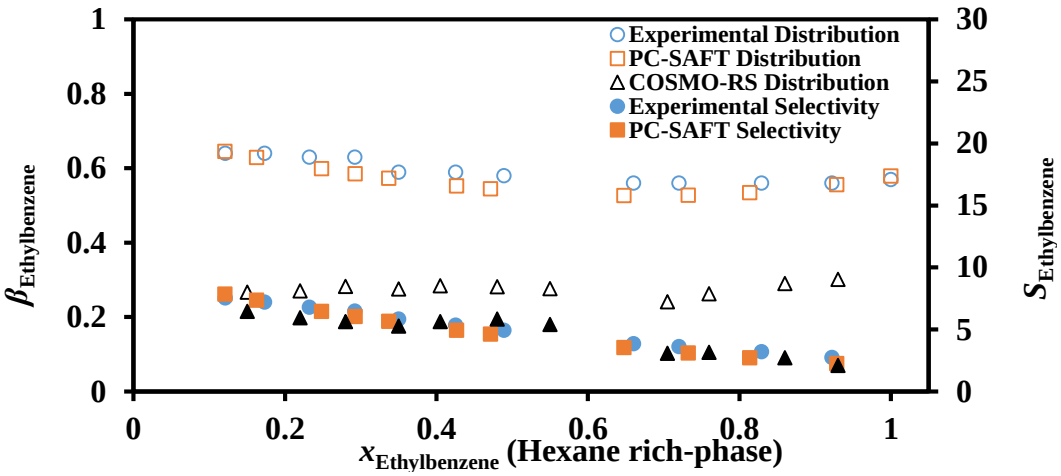

Figure 5. Comparison between the experimental [20] and calculated distribution coefficient and selectivity by PC-SAFT and COSMO-RS [20] models as a function of ethylbenzene mole fraction in n-hexane rich-phase (T=298.15 K, P=101.3 kPa).

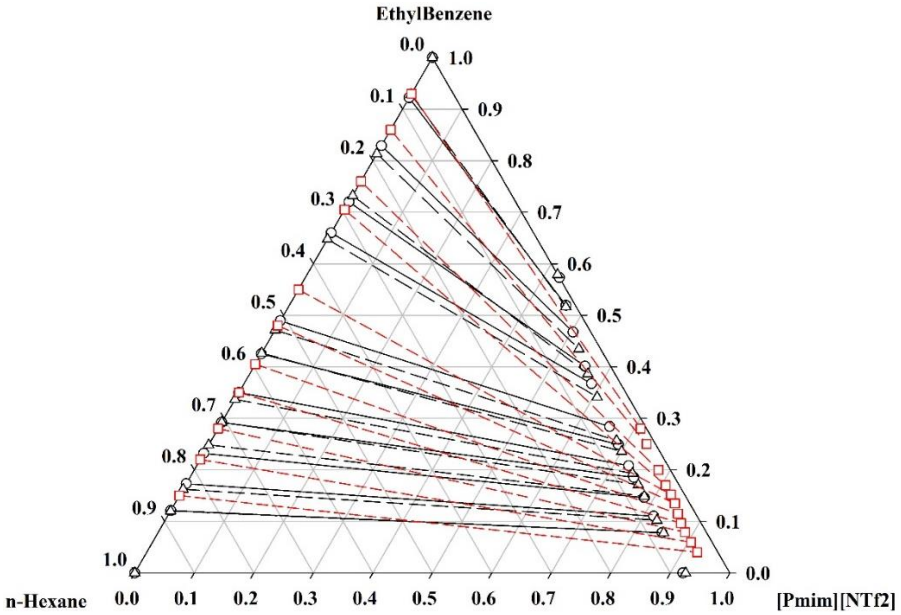

Figure 6. LLE data for the system of n-hexane + ethylbenzene + [Pmim][NTf_2]. Comparison between the experimental [20] (solid black lines) and calculated compositions by PC-SAFT

(dashed black lines) and COSMO-RS [20] models (dashed red lines) at T=298.15 K and P=101.3 kPa.

4.4. Modeling LLE of the ternary system of heptane + thiophene + [COC_2mPYR][NTf_2].

The triangular diagram associated with the compositions of the experimental tie-lines for the ternary system of n-heptane + thiophene + 1-(2-methoxyethyl)-1-methylpyrrolidinium bis(trifluoromethylsulfonyl)-amide) [COC_2mPYR][NTf_2] at 298.15 K was shown in Figure 7. As can be seen, comparisons have been made between PC-SAFT and NRTL models with experimental data. The RMSD of the PC-SAFT and NRTL models are 2.451% and 0.34%, respectively. The selectivity S and solute distribution ratio β values of the ternary system, according to Eqs. 7 and 8, were displayed in Figure 8. The ARD of the distribution coefficient and selectivity of the two models are 9.437%/16.809% and 0.961%/6.346%, respectively. Solute distribution ratios are higher than unity, which resembles the effectiveness of the IL to extract thiophene from its mixture with n-heptane, however, β values decrease as solute concentration increases in the aliphatic rich-phase.

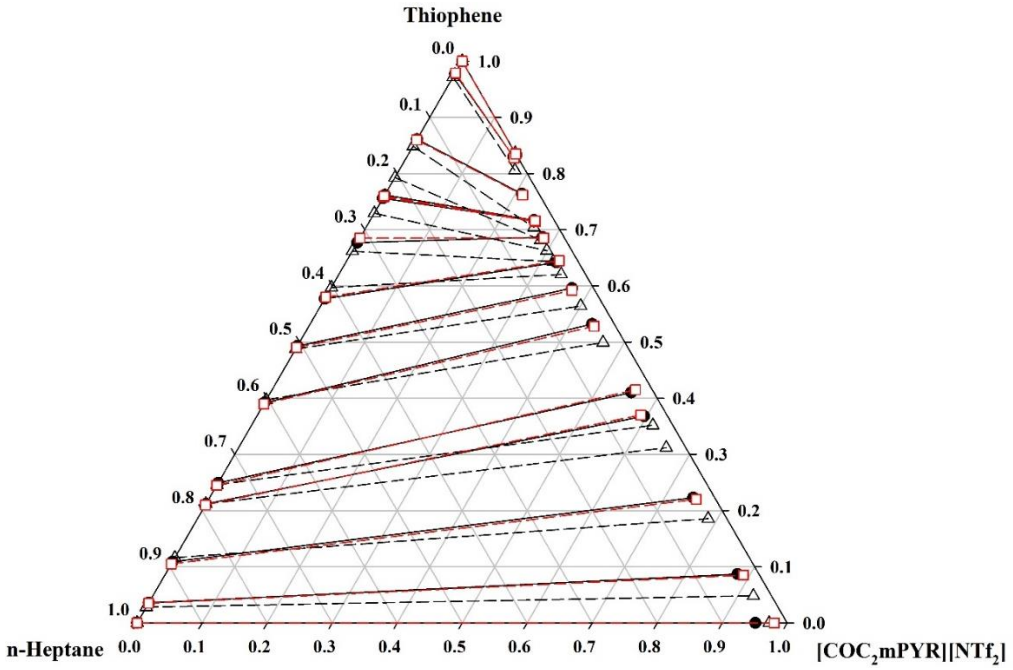

Figure 7. LLE data for the system of n-heptane + thiophene + [COC_2mPYR][NTf_2]. Comparison between the experimental [38] (solid black lines) and calculated compositions by PC-SAFT (dashed black lines) and NRTL [38] models (dashed red lines) at T=298.15 K and P=101.3 kPa. PC-SAFT pure-component parameters of the [COC_2mPYR][NTf_2] were obtained by fitting to the experimental liquid density data [39], as one can neglect the vapor pressure values of the ILs. The *ARDρ* of 2.097% shows the accuracy of the PC-SAFT to predict liquid density data over wide ranges of temperature. Figure S6 of the Supplementary Material associated with this study shows the predicted liquid density of [COC_2mPYR][NTf_2]. Also, binary interaction parameters k_{ij} were obtained through fitting to the ternary LLE data and were displayed in Table 3. Levenberg Marquardt algorithm with the initial guess of k_{ij} = 0 was used for the optimization of the binary interaction parameters, which show stronger interactions between [COC_2mPYR][NTf_2] and thiophene compared to n-heptane.

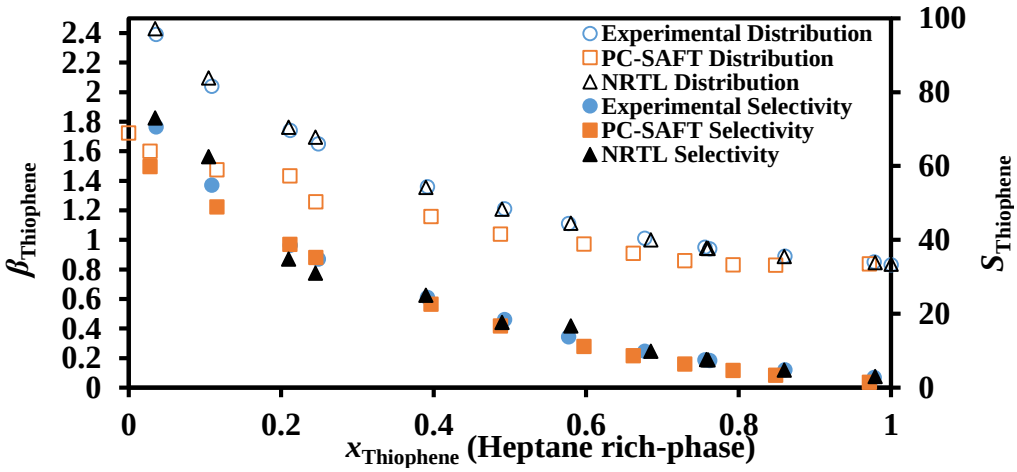

Figure 8. Comparison between the experimental [38] and calculated distribution coefficient and selectivity by PC-SAFT and NRTL [38] models as a function of thiophene mole fraction in n-heptane rich-phase (T=298.15 K, P=101.3 kPa).

Investigation of the β and S values in Figures 2, 3, 5, and 8 show that lengthier cation or introduction of an oxygen moiety into the cation molecular structure favors the high performance extraction of aromatic compounds from their aliphatics counterpart.

4.5. Modeling VLE of the binary systems of CO_2 + Ether-Functionalized or nonfunctionalized Pyridinium ILs.

PC-SAFT modeling of CO_2 and CH_4 solubilities in $[E_nPy][NTf_2]$ and $[C_mPy][NTf_2]$ over the temperature range of 313.15-333.15 K were displayed in Figures 9 and 10, respectively. Clearly, methane solubility in the six ILs is much lower than the solubility of carbon dioxide, which signifies the application of these ILs to selectively absorb CO_2 from its mixture with CH_4. From binary interaction parameters in Table 3, $[E_2Py][NTf_2]$ and $[E_3Py][NTf_2]$ are more efficient for selective absorption of CO_2 from its mixture with CH_4 compared to their counterparts of nonfunctionalized pyridinium ILs $[C_7Py][NTf_2]$ and $[C_{10}Py][NTf_2]$. Also, in terms of selectivity, lengthier cation part and more ether oxygen atoms favor CO_2 absorption. However, increasing the temperature will decrease the CO_2 and CH_4 solubilities in both $[E_nPy][NTf_2]$ and $[C_mPy][NTf_2]$ ILs, while the rate of decline in CO_2 solubility is more than CH_4 solubility does. For instance, increasing the temperature from 313.15 K to 333.15 K will decrease CO_2 solubility in $[E_3Py][NTf_2]$ almost 29%, while CH_4 solubility decreases 12.9% over the same temperature shift. The ARDP% for the six ILs modeled by PC-SAFT was provided in Table 4. As can be seen, PC-SAFT model results are in good qualitative agreement with the experimental data [7].

Table 4. ARDP% values of the PC-SAFT model for the six ILs over the temperature range of 313.15-333.15 K.

IL / Gas	$[C_4Py][NTf_2]$	$[C_7Py][NTf_2]$	$[C_{10}Py][NTf_2]$	$[E_1Py][NTf_2]$	$[E_2Py][NTf_2]$	$[E_3Py][NTf_2]$
CO_2	4.809	10.537	7.681	7.090	13.574	8.692
CH_4	7.630	4.884	10.481	6.715	9.384	8.338

Since CO_2 and CH_4 molecules were considered non-associating, no cross-association allowed between molecules. A...B association scheme in the ILs was accounted for the six ILs, while 0.01 and 1×10^{-6} values for the association volume and 5000 K for the association energy were used for the ILs. These values are common for the consideration of association interactions in ILs [10].

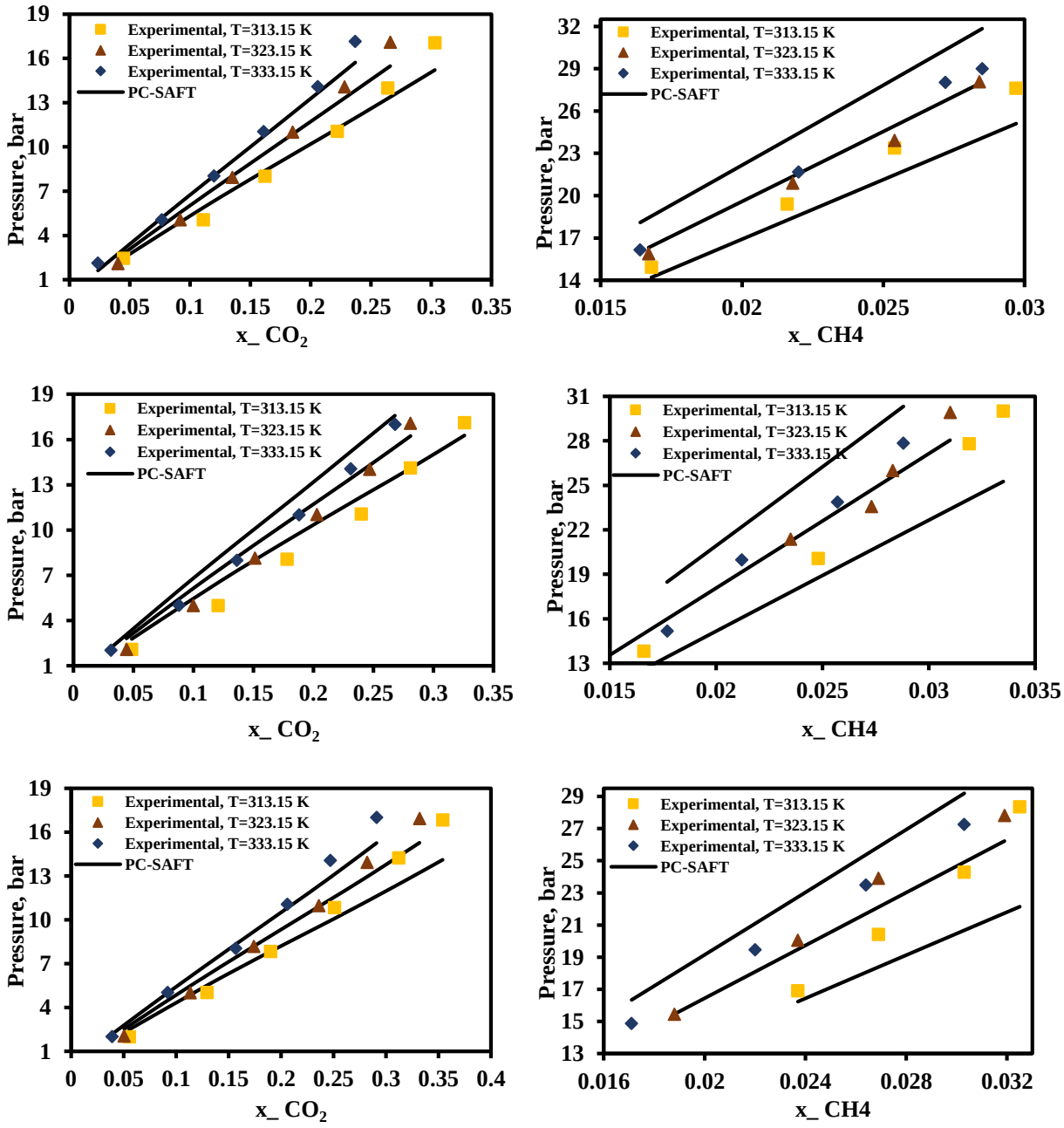

Figure 9. CO_2 and CH_4 solubilities in $[E_nPy][NTf_2]$ (n=1,2,3) at various temperatures. From up to bottom: $[E_1Py][NTf_2]$, $[E_2Py][NTf_2]$, and $[E_3Py][NTf_2]$. Points are experimental data [7] and solid lines are PC-SAFT modeling.

The PC-SAFT pure-component parameters of the six ILs and the ARDρ% associated with the fitting procedure to the experimental liquid density data [7] were tabulated in Table 2. Supplementary Material dealing with this article contains the predictions of the liquid density data and comparisons to the experimental values for the studied ILs. Temperature-independent binary interaction parameters were used for the ILs + CO_2 systems, and temperature-dependent k_{ij}s were used for the ILs + CH_4 systems by fitting to the experimental VLE data [7].

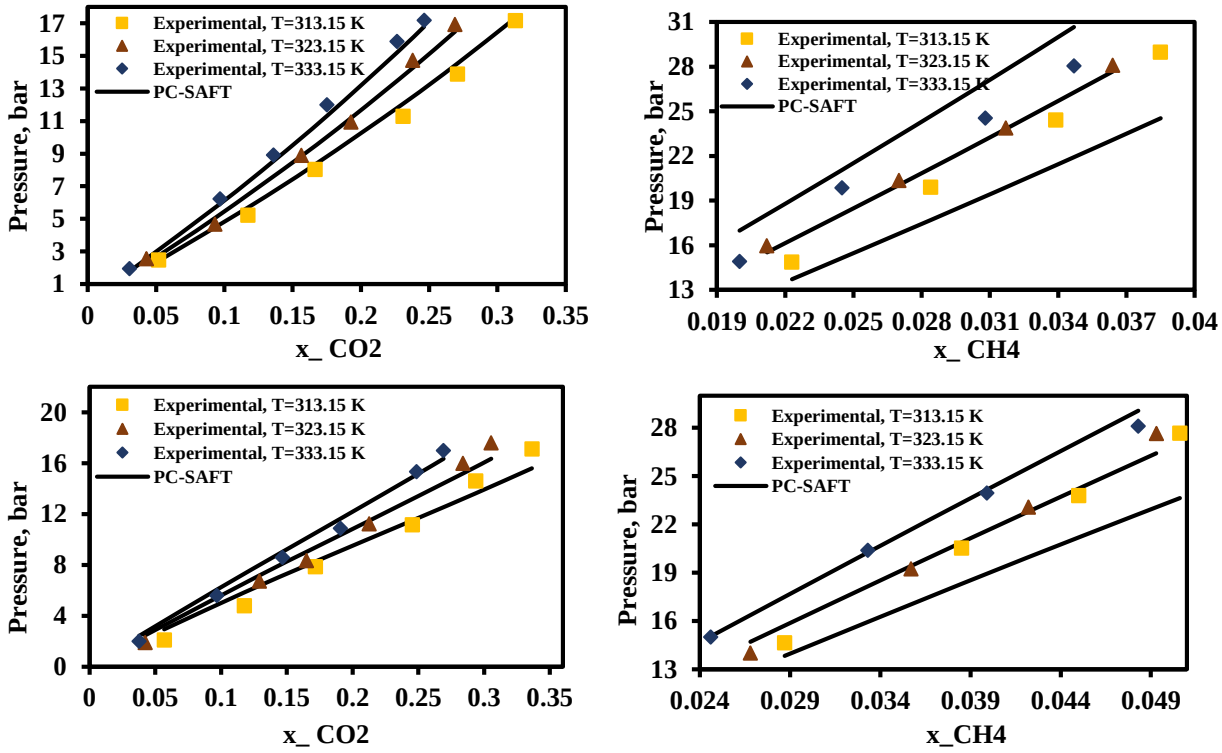

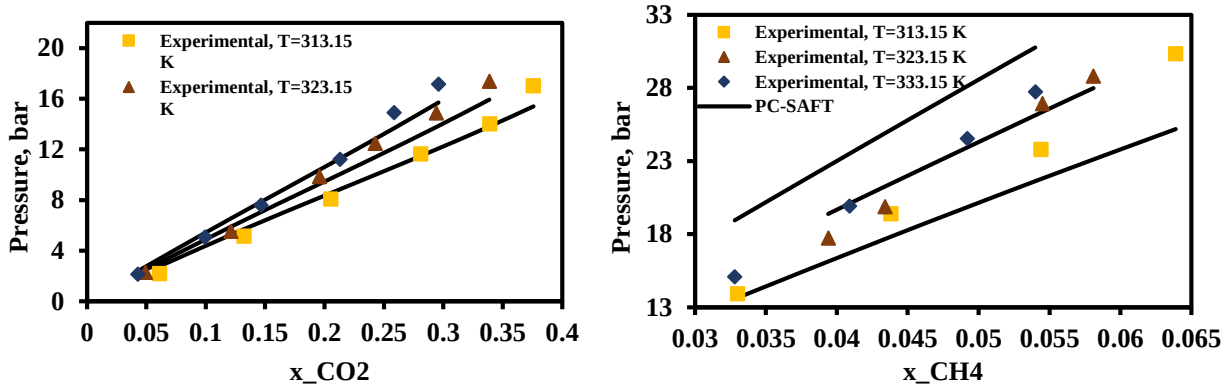

Figure 10. CO_2 and CH_4 solubilities in $[C_nPy][NTf_2]$ (n=4,7,10) at various temperatures. From up to bottom: $[C_4Py][NTf_2]$, $[C_7Py][NTf_2]$, and $[C_{10}Py][NTf_2]$. Points are experimental data [7] and solid lines are PC-SAFT modeling.

Under vacuum operation and at higher temperatures CO_2 desorption can be happened, and it has been shown that these ILs can be regenerated and reused multiple times [7]. Addition of water can reduce the high viscosity of the ILs, while water content could reduce the amount of CO_2 absorbed primarily due to the decrease in the IL concentration. PC-SAFT model has been used to model the VLE of the ternary system of IL + CO_2 + water [32]. Addition of water could increase the operational pressure of the system, which can be calculated from PC-SAFT formulation, as another advantage of this modeling approach for precise design purposes.

4.6. Modeling VLE of the binary systems of C_4H_{10} + C_4F_{10} or C_6H_{14} + C_6F_{14}.

Predicted liquid density and vapor pressure of n-perfluorobutane (C_4F_{10}) as a function of temperature were shown in the Supplementary Material associated with this article (Figures S14 and 15). As shown, the densities decrease with the increase of temperature. According to Eq. (6), $ARD\rho\%$ and $ARDp^{sat}\%$ of 1.956 and 0.613% were obtained during optimization of the PC-SAFT parameters of the pure component of C_4F_{10}. n-Perfluorobutane was considered with dipolar interactions, although polar contribution to the PC-SAFT model of the pure-component was found to be minor. PC-SAFT pure-component parameters of the n-perfluorohexane (C_6F_{14}) were used

from the previous work [32], while PC-SAFT model parameters of the n-butane and n-hexane were taken from Gross and Sadowski [29]. According to the sigma-profile of the electrical charge distribution of the bodies in Figure 11, the mixture of C_4H_{10} + C_4F_{10} almost repel each other and the unlike interactions are more dominant. Therefore, positive deviations from Raoult's law with positive activity coefficients are the proof of such interactions. For the preparation of the sigma-profiles of the components, the VT-2005 sigma-profile database of Mullins was used [46].

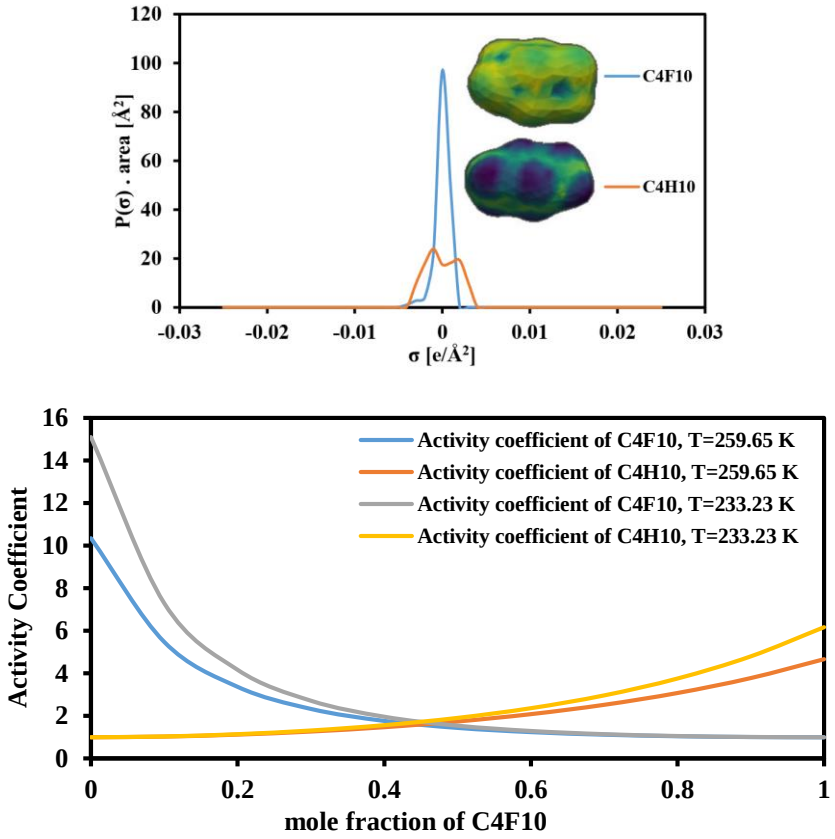

Figure 11. Sigma-profile (upper) and activity coefficients (lower) of the mixture of C_4H_{10} + C_4F_{10}.

Figure 12 shows four VLE isotherms of the binary mixture of C_4H_{10} + C_4F_{10} and comparisons between PC-SAFT and SAFT-γ Mie [27] predictions with experimental data [40]. The theoretical calculations of the PC-SAFT are in good agreement with experimental data over the entire mole

fractions of C_4F_{10}, specifically reproducing the azeotropic compositions and the abnormal flat shape of the isotherms, however, SAFT-γ Mie underpredicted the experimental trends for the whole isotherms with the total vapor pressure predictions of nearly 7%. PC-SAFT with temperature dependent binary interaction parameter produces ARDP and ARDy of 1.262% and 2.261%, respectively, while ARDP and ARDy of the SAFT-γ Mie are 5.119% and 2.732%, respectively. The main advantage of the SAFT-γ Mie would be its transferability to other n-alkane/perfluoro-n-alkane systems because it is based on the group contribution of alkyl and perfluoroalkyl segments. However, one needs to estimate the whole functional group parameters and it has six fitting parameters.

Similarly, Figure 13 represents the three VLE isotherms of the binary mixture of C_6H_{14} + C_6F_{14}. Comparisons were made against SAFT-γ Mie [27] and GC-SAFT-VR [47], which are pure predictive models, with experimental data [48]. Predictions were made at three different temperatures ranging from 298.15 to 318.15 K. As shown, by increasing temperature the deviation between experimental and calculated pressures and vapor mole fractions by other two models increases too, while the proposed PC-SAFT model correctly predicts the azeotrope points and the whole phase envelope. The ARDP/ARDy of PC-SAFT, SAFT-γ Mie, and GC-SAFT-VR are 2.814/3.599%, 7.10/4.023%, and 8.420/4.099%, respectively. Like SAFT-γ Mie, once GC-SAFT-VR is constructed it can be transferred to similar systems, but it needs higher fitting parameters in comparison to the PC-SAFT model.

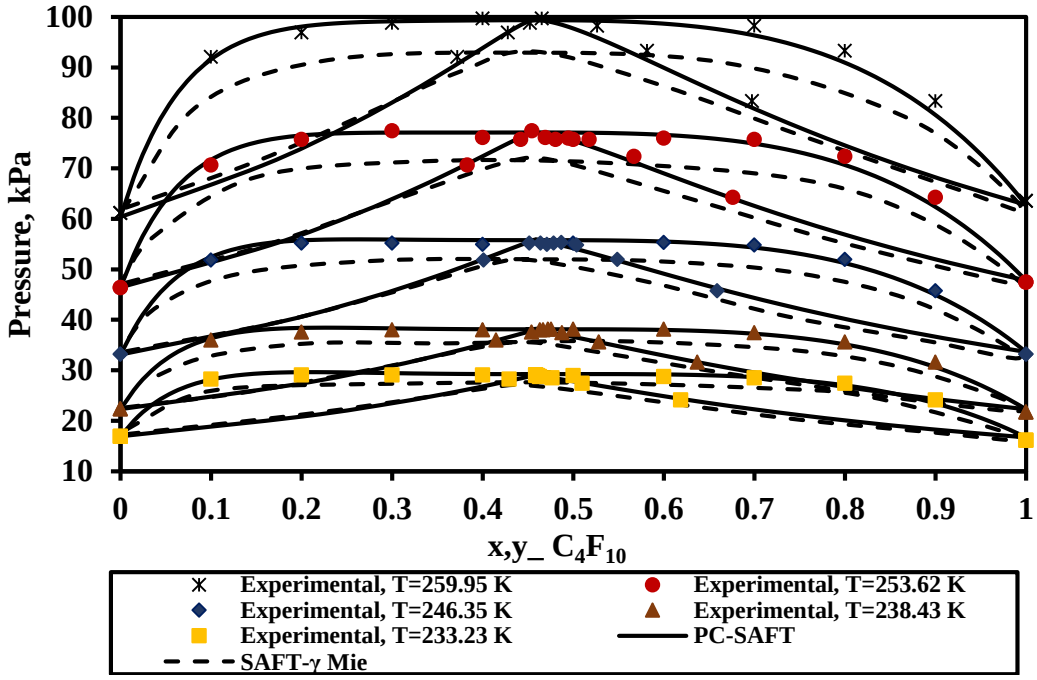

Figure 12. Comparison between the experimental [40] and calculated VLE data by PC-SAFT and molecular thermodynamic model [27] for C_4F_{10}-C_4H_{10} mixture.

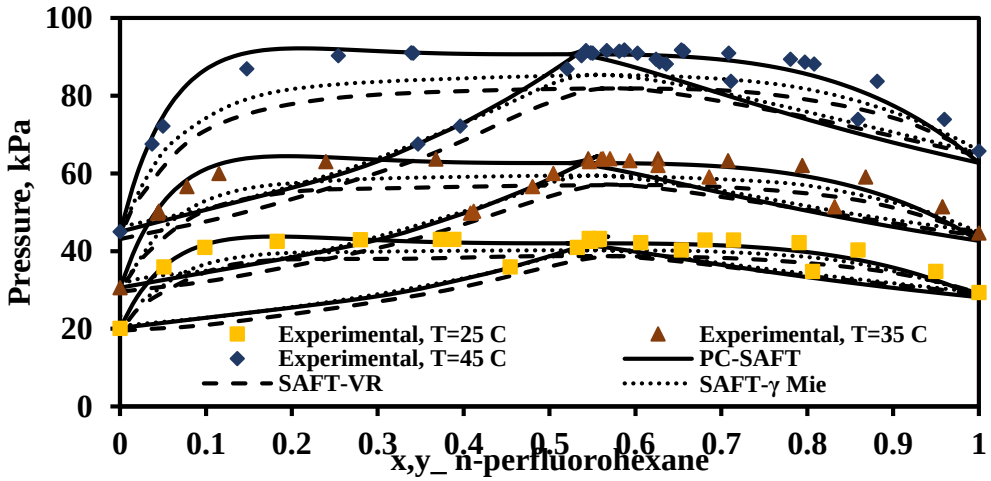

Figure 13. Comparison between the experimental [48] and calculated VLE data by PC-SAFT and molecular thermodynamic models [27,47] for C_6F_{14}-C_6H_{14} mixture.

5. Conclusions

PC-SAFT was used to model the LLE of ILs or DESs for the separation of aromatics from aliphatics. The DESs were tetrabutylammonium chloride/levulinic acid (1:2) and

tetrabutylammonium bromide/diethylene glycol (1:4), while ILs were 1-propyl-3-methylimidazolium bis{trifluoromethylsulfonyl}imide and 1-(2-methoxyethyl)-1-methylpyrrolidinium bis(trifluoromethylsulfonyl)-amide). Also, VLE modeling of the binary mixtures of CO_2 + ether-functionalized or nonfunctionalized pyridinium ILs were performed. Finally, VLE modeling of the binary mixtures of C_4F_{10} + C_4H_{10} or C_6H_{14} + C_6F_{14} were considered, as the mixtures exhibit positive deviation from Raoult's law. For the LLE systems, comparisons have been made against COSMO-RS and NRTL models, which showed quite robustness of the proposed PC-SAFT model with the pure-component parameters developed in this study. It was observed that application of DESs and ILs for liquid extraction are promising, although there might be a need for multiple recovery and reuse due to the low values of the distribution coefficients. Temperature-dependent and independent binary interaction parameters were used to increase the accuracy of the modeling for the systems considered in this work. An average RMSD values of 2.206% for the LLE systems, an average ARDP of 7.420% for the ILs + CO_2 or CH_4 and perfluoroalkane + alkane systems, and an average ARDy of 2.930% for perfluoroalkane + alkane systems were obtained.

AUTHOR INFORMATION

Corresponding Author

Ali Aminian - *Institute of Thermomechanics of the Czech Academy of Sciences, Dolejškova 5, 182 00 Czech Republic;* orcid.org/0000-0002-2072-3543; Email: aminian@it.cas.cz

Notes

The author declares no competing financial interest.

References

[1] M. Królikowski, M. Królikowska, C. Wiśniewski, Separation of aliphatic from aromatic hydrocarbons and sulphur compounds from fuel based on measurements of activity coefficients at

infinite dilution for organic solutes and water in the ionic liquid N,N-diethyl-N-methyl-N-(2-methoxy-ethyl)ammonium bis (trifluoromethylsulfonyl)imide, J. Chem. Thermodyn. 103 (2016) 115-124.

[2] N.R. Rodriguez, T. Gerlach, D. Scheepers, M.C. Kroon, I. Smirnova, Experimental determination of the LLE data of systems consistingof {hexane + benzene + deep eutectic solvent} and prediction using the Conductor-like Screening Model for Real Solvents, J. Chem. Thermodyn. 104 (2017) 128-137.

[3] E.L. Smith, A.P. Abbott, K.S. Ryder, Deep eutectic solvents (DESs) and their applications, Chem. Rev. 114 (2014) 11060-11082.

[4] M.L. Alcantara, P.I.S. Ferreira, G.O. Pisoni, A.K. Silva, L. Cardozo-Filho, L.M. Lião, C.A.M. Pires, S. Mattedi, High pressure vapor-liquid equilibria for binary protic ionic liquids + methane or carbon dioxide, Sep. Purif. Technol. 196 (2018) 32-40.

[5] M. Ramdin, A. Amplianitis, S. Bazhenov, A. Volkov, V. Volkov, T.J.H. Vlugt, T.W. de Loos, Solubility of CO_2 and CH_4 in ionic liquids: Ideal CO_2/CH_4 selectivity, Ind. Eng. Chem. Res. 53 (2014) 15427-15435.

[6] S.D. Hojniak, I.P. Silverwood, A. Laeeq Khan, I.F.J. Vankelecom, W. Dehaen, S.G. Kazarian, K. Binnemans, Highly selective separation of carbon dioxide from nitrogen and methane by nitrile/glycol-difunctionalized ionic liquids in supported ionic liquid membranes (SILMs), J. Phys. Chem. B 118 (2014) 7440-7449.

[7] S. Zeng, J. Wang, L. Bai, B. Wang, H. Gao, D. Shang, X. Zhang, S. Zhang, Highly selective capture of CO_2 by ether-functionalized pyridinium ionic liquids with low viscosity, Energ. Fuel 29 (2015) 6039-6048.

[8] X. Zhang, W. Xiong, L. Peng, Y. Wu, X. Hu, Highly selective absorption separation of H_2S and CO_2 from CH_4 by novel azole-based protic ionic liquids. AIChE J. 66 (2020) 16936.

[9] M. Ramdin, T.Z. Olasagasti, T.J.H. Vlugt, T.W. de Loos, High pressure solubility of CO_2 in non-fluorinated phosphonium-based ionic liquids, J. Supercrit. Fluid 82 (2013) 41-49.

[10] A. Nann, C. Held, G. Sadowski, Liquid-liquid equilibria of 1-butanol/water/IL systems, Ind. Eng. Chem. Res. 52 (2013) 18472-18481.

[11] H. Al-fnaish, L Lue, Modelling the solubility of H_2S and CO_2 in ionic liquids using PC-SAFT equation of state, Fluid Phase Equilib. 450 (2017) 30-41.

[12] L.F. Zubeir, C. Held, G. Sadowski, M.C. Kroon, PC-SAFT modeling of CO_2 solubilities in deep eutectic solvents, J. Phys. Chem. B 120 (2016) 2300-2310.

[13] R.I. Canales, C. Held, M.J. Lubben, J.F. Brennecke, G. Sadowski, Predicting the solubility of CO_2 in toluene + ionic liquid mixtures with PC-SAFT, Ind. Eng. Chem. Res. 56 (2017) 9885-9894.

[14] K. Paduszynski, E.V. Lukoshko, M. Królikowski, U. Domanska, Measurements and equation of-state modelling of thermodynamic properties of binary mixtures of 1-butyl-1-methylpyrrolidinium tetracyanoborate ionic liquid with molecular compounds, J. Chem. Thermodyn. 90 (2015) 317-326.

[15] A.S.L. Gouveia, F.S. Oliveira, K.A. Kurnia, I.M. Marrucho, Deep eutectic solvents as azeotrope breakers: liquid-liquid extraction and COSMO-RS prediction, ACS Sustain. Chem. Eng. 4 (2016) 5640-5650.

[16] S.E.E. Warrag, N.R. Rodriguez, I.M. Nashef, M. van Sint Annaland, J.I. Siepmann, M.C. Kroon, C.J. Peters, Separation of thiophene from aliphatic hydrocarbons using tetrahexylammonium-based deep eutectic solvents as extracting agents, J. Chem. Eng. Data 62 (2017) 2911-2919.

[17] M.A. Kareem, F.S. Mjalli, M.A. Hashim, M.K.O. Hadj-Kali, F.S. Ghareh Bagh, I.M. Al nashef, Phase equilibria of toluene/heptane with deep eutectic solvents based on ethyltriphenylphosphonium iodide for the potential use in the separation of aromatics from naphtha, J. Chem. Thermodyn. 65 (2013) 138-149.

[18] S. Mulyono, H.F. Hizaddin, I. Wazeer, O. Alqusair, E. Ali, M.A. Hashim, M. K. Hadj-Kali, Liquid-liquid equilibria data for the separation of ethylbenzene/styrene mixtures using ammonium-based deep eutectic solvents, J. Chem. Thermodyn. 135 (2019) 296-304.

[19] S. Corderí, N. Calvar, E. Gómez, A. Domínguez, Capacity of ionic liquids [EMim][NTf_2] and [EMpy][NTf_2] for extraction of toluene from mixtures with alkanes: Comparative study of the effect of the cation, Fluid Phase Equilib 315 (2012) 46-52.

[20] I. Domínguez, E.J. González, J. Palomar, Á. Domínguez, Phase behavior of ternary mixtures {aliphatic hydrocarbon + aromatic hydrocarbon + ionic liquid}: Experimental LLE data and their modeling by COSMO-RS, J. Chem. Thermodyn. 77 (2014) 222-229.

[21] N. Calvar, I. Domínguez, E. Gómez, J. Palomar, Á. Domínguez, Evaluation of ionic liquids as solvent for aromatic extraction: Experimental, correlation and COSMO-RS predictions, J. Chem. Thermodyn. 67 (2013) 5-12.

[22] M. Durski, P. Naidoo, D. Ramjugernath, U. Domanska, Ternary liquid-liquid phase equilibria of {ionic liquid + thiophene + (octane/hexadecane)}, J. Chem. Thermodyn. 134 (2019) 157-163.

[23] S.E.E. Warrag, I. Adeyemi, N.R. Rodriguez, I.M. Al nashef, M. van Sint Annaland, M.C. Kroon, C.J. Peters, Effect of the type of ammonium salt on the extractive desulfurization of fuels using deep eutectic solvents, J. Chem. Eng. Data 63 (2018) 1088-1095.

[24] E. Cea-Klapp, I. Polishuk, R.I. Canales, H. Quinteros-Lama, J.M. Garrido, Estimation of thermodynamic properties and phase equilibria in systems of deep eutectic solvents by PC-SAFT EoS, Ind. Eng. Chem. Res. 59 (2020) 22292-22300.

[25] S.E.E. Warrag, C. Pototzki, N.R. Rodriguez, M. van Sint Annaland, M.C. Kroon, C. Held, G. Sadowski, C.J. Peters, Oil desulfurization using deep eutectic solvents as sustainable and economical extractants via liquid-liquid extraction: Experimental and PC-SAFT predictions, Fluid Phase Equilib. 467 (2018) 33-44.

[26] C. McCabe, A. Galindo, A. Gil-Villegas, G. Jackson, Predicting the high-pressure phase equilibria of binary mixtures of Perfluoro-n-alkanes + n-Alkanes using the SAFT-VR approach, J. Phys. Chem. B 102 (1998) 8060-8069.

[27] P. Morgado, J. Barras, A. Galindo, G. Jackson, E.J.M. Filipe, Modeling the fluid-phase equilibria of semifluorinated alkanes and mixtures of (n-Alkanes + n-Perfluoroalkanes) with the SAFT-γ Mie group-contribution approach, J. Chem. Eng. Data 65 (2020) 5909-5919.

[28] S. Aparicio, Phase equilibria in perfluoroalkane + alkane binary systems from PC-SAFT equation of state, J. Supercrit. Fluid 46 (2008) 10-20.

[29] J. Gross, G. Sadowski, Perturbed-chain SAFT: An equation of state based on a perturbation theory for chain molecules, Ind. Eng. Chem. Res. 40 (2001) 1244-1260.

[30] J. Gross, G. Sadowski, Application of the perturbed-chain SAFT equation of state to associating systems, Ind. Eng. Chem. Res. 41 (2002) 5510-5515.

[31] P.K. Jog, W.G. Chapman, Application of Wertheim's thermodynamic perturbation theory to dipolar hard sphere chains, Mol. Phys. 97 (1999) 307-319.

[32] A. Aminian, Modeling the Vapor-Liquid equilibria of binary and ternary systems comprising associating and non-Associating compounds by using Perturbed-Chain Statistical association fluid Theory. Part I, J. Chem. Thermodyn. 162 (2021) 106563.

[33] H. Wang, Y. Wu, W. Dong, A study of densities and volumetric properties of binary mixtures containing nitrobenzene at T = (293.15 to 353.15) K, J. Chem. Thermodyn., 2005, 37, 866-886.

[34] W. Patnode, W.J. Scheiber, The density, thermal expansion, vapor pressure, and refractive index of styrene, and the density and thermal expansion of polystyrene, J. Am. Chem. Soc. 61 (1939) 3449-3451.

[35] H. Wang, W. Liu, Y. Wu, Effect of temperature on the volumetric properties of (cyclohexanone + an aromatic hydrocarbon), J. Chem. Thermodyn. 36 (2004) 1079-1087.

[36] D.M. von Niederhausern, G.M. Wilson, N.F. Giles, Critical point and vapor pressure measurements at high temperatures by means of a new apparatus with ultralow residence times, J. Chem. Eng. Data 45 (2000) 157-160.

[37] M.A.A. Rocha, C.M.S.S. Neves, M.G. Freire, O. Russina, A. Triolo, J.A.P. Coutinho, L.M.N.B.F. Santos, Alkylimidazolium based ionic liquids: impact of cation symmetry on their nanoscale structural organization, J. Phys. Chem. B 117 (2013) 10889-10897.

[38] A. Marciniak, M. Królikowski, Ternary liquid–liquid equilibria of bis(trifluoromethylsulfonyl)-amide based ionic liquids + thiophene + n-heptane. The influence of cation structure, Fluid Phase Equilib. 321 (2012) 59-63.

[39] F.M. Gacino, T. Regueira, L. Lugo, M.J.P. Comunas, J. Fernandez, Influence of molecular structure on densities and viscosities of several ionic liquids, J. Chem. Eng. Data 56 (2011) 4984-4999.

[40] J. H. Simons, J. W. Mausteller, The properties of N-Butforane and its mixtures with n-Butane, J. Chem. Phys. 20 (1952) 1516-1519.

[41] R. D. Fowler, J.M. Hamilton, J.S. Kasper, C.E. Weber, W.B. Burford, H.C. Anderson, Physical and chemical properties of pure fluorocarbons, Ind. Eng. Chem. 39 (1947) 375-378.

[42] J.A. Brown, W.H. Mears, Physical properties of n-Perfluorobutane, J. Phys. Chem. 62 (1958) 960-962.

[43] H.G. Rackett, Equation of state for saturated liquids, J. Chem. Eng. Data 15 (1970) 514-517.

[44] M. Karpińska, U. Domańska, M. Wlazło, Separation of ethylbenzene/styrene systems using ionic liquids in ternary LLE, J. Chem. Thermodyn. 103 (2016) 423-431.

[45] A.P. Carneiro, C. Held, O. Rodriguez, G. Sadowski, M.E.R.A. Macedo, Solubility of sugars and sugar alcohols in ionic liquids: measurement and PC-SAFT modeling, J. Phys. Chem. B 117 (2013) 9980-9995.

[46] E. Mullins, R. Oldland, Y.A. Liu, S. Wang, S.I. Sandler, C-C. Chen, M. Zwolak, K. Seavey, Sigma-profile database for using COSMO-based thermodynamic methods, Ind. Eng. Chem. Res. 45 (2006) 3973-3999.

[47] J.D. Haley, C. McCabe, Predicting the phase behavior of fluorinated organic molecules using the GC-SAFT-VR equation of state, Fluid Phase Equilib. 440 (2017) 111-121.

[48] R.D Dunlap, R.G. Bedford, J.C. Woodbrey, S.D. Furrow, Liquid-vapor equilibrium for the system: Perfluoro-n-Hexane – nHexane, J. Am. Chem. Soc. 81 (1959) 2927-2930.